Pflügers Arch – Eur J Physiol (1998) 436:757–765

ORIGINAL ARTICLE

Richard Fleischhauer · Nenad Mitrovic
Feza Deymeer · Frank Lehmann-Horn · Holger Lerche

Effects of temperature and mexiletine on the F1473S Na^+ channel mutation causing paramyotonia congenita

Received: 13 January 1998 / Received after revision: 11 May 1998 / Accepted: 19 May 1998

Abstract The F1473S mutation of the adult human skeletal muscle Na^+ channel causes paramyotonia congenita, a disease characterized by muscle stiffness sometimes followed by weakness in a cold environment. The symptoms are relieved by the local anaesthetic mexiletine. This mutation, which resides in the cytoplasmic S4-S5 loop in domain IV of the α-subunit, was studied by heterologous expression in HEK293 cells using standard patch-clamp techniques. Compared to wild-type (WT) channels, those with the F1473S mutation exhibit a twofold slowing of fast inactivation, an increased persistent Na^+ current, a +18-mV shift in steady-state inactivation and a fivefold acceleration of recovery from fast inactivation; slow inactivation was similar for both clones. Single-channel recordings for the F1473S mutation revealed a prolonged mean open time and an increased number of channel reopenings that increased further upon cooling. The pharmacological effects of mexiletine on cells expressing either WT, F1473S or G1306E channels were studied. G1306E is a myotonia-causing mutation located within the inactivation gate that displays similar but stronger inactivation defects than F1473S. The hyperpolarizing shift in steady-state inactivation induced by mexiletine was almost identical for all three clones. In contrast, this agent had a reduced effectiveness on the phasic (use-dependent) block of Na^+ currents recorded from the mutants: the relative order of block was WT>F1473S>G1306E. We suggest that the relative effectiveness of mexiletine is associated with the degree of abnormal channel inactivation and that the relative binding affinity of mexiletine is not substantially different between the mutations or the WT.

Key words Human skeletal muscle · Inactivation · Ion channel · Local anaesthetic · Myotonia · Patch-clamp · Pharmacology

R. Fleischhauer · N. Mitrovic · F. Lehmann-Horn · H. Lerche (✉)
Department of Applied Physiology, University of Ulm, D-89069 Ulm, Germany
e-mail: holger.lerche@medizin.uni-ulm.de
Tel.: +49-731-5023250, Fax: +49-731-5033609

N. Mitrovic · H. Lerche
Department of Neurology, University of Ulm, D-89069 Ulm, Germany

F. Deymeer
Department of Neurology, Istanbul University, CAPA 34390, Istanbul, Turkey

Introduction

Normal gating of Na^+ channels is required for the generation and propagation of action potentials in nerve and muscle cells. Na^+ channels open briefly upon membrane depolarization and then close to a fast inactivated state from which they reopen only rarely. Thus, fast inactivation limits the duration of an action potential and also initiates its repolarizing phase. Subsequent to an action potential, the excitable membranes become refractory for a short period of time. This refractory period limits the firing rate of a muscle or nerve fibre and is regulated primarily by the recovery of Na^+ channels from inactivation.

The gating of Na^+ channels is changed in three autosomal dominant muscle diseases, hyperkalaemic periodic paralysis (HyperPP), paramyotonia congenita (PC), and potassium-aggravated myotonia (PAM). All have been shown to be caused by distinct point mutations within the α-subunit of the adult human skeletal muscle Na^+ channel. To date, about 20 mutations are known to cause these so-called Na^+ channelopathies [14]. PC is phenotypically characterized by paradoxical myotonia, i.e. muscle stiffness increasing upon repeated activity (in contrast to the "warm-up" phenomenon seen with chloride channel myotonia) and a significant temperature dependence of symptoms. Muscle stiffness occurs predominantly in a cold environment and sometimes gives way to flaccid weakness after a prolonged exposure to cold [18]. The investigated patient, carrying the mutation F1473S, showed all these classic symptoms. In contrast, temperature dependence is not a typical clinical feature of either PAM or HyperPP. The hallmark of HyperPP is

episodic weakness sometimes accompanied by myotonia, whereas PAM is characterized by muscle stiffness induced and aggravated by depolarizing agents such as potassium, typically without weakness.

Voltage-clamp experiments on native or cultured samples of biopsied muscle from patients with Na^+ channelopathies revealed incomplete Na^+ channel inactivation as a common underlying pathology [5, 15–17, 19, 20]. Expression of mutant Na^+ channels in heterologous systems confirmed these results, but also revealed more detailed features of Na^+ channel dysfunction, such as a shift in gating modes, accelerated recovery from inactivation, increase in "window current", uncoupling of activation from inactivation and/or impaired slow inactivation [4, 7, 8, 11, 24–26, 33]. Alteration of inactivation increases the Na^+ inward current which depolarizes the muscle membrane and can cause either hyperexcitability (mild depolarization→myotonia) or inexcitability (strong depolarization→paralysis).

The functionally important α-subunit of the Na^+ channel consists of four highly homologous domains (I–IV), each containing six transmembrane segments (S1–S6). The S5–S6 loops form the ion-selective pore, the S4 segments contain positively charged residues conferring voltage dependence to the protein and the III–IV cytoplasmic linker contains the supposed inactivation gate of the channel [6]. The mutated amino acid F1473, causing PC, is located within the intracellular loop between segments S4 and S5 of the fourth domain (IV/S4–S5). In previous/parallel studies of our and other groups it has been shown that mutations of F1473 and other amino acids in IV/S4–S5 strongly affect fast inactivation and that the secondary structure of this loop is most probably an α-helix [10, 21, 23, 26]. Via its attachment to the voltage sensor IV/S4 [34], the IV/S4–S5 segment may play a crucial role in the conformational change associated with receptor formation for the putative inactivation particle, thereby coupling inactivation to activation.

The first aim of our study was to provide a detailed characterization of the underlying biophysical defect of the F1473S mutant. To do so, we employed whole-cell and single-channel patch-clamp techniques to study transfected HEK-293 cells. In a previously published report, we present the macroscopic defects of fast inactivation that occur following this naturally occurring mutation in comparison to those that result from other engineered mutations in the same channel region. The aim of the previous study was to determine the role in fast inactivation of conserved amino acids among Na^+ and K^+ channels in the IV/S4–S5 loop. In those investigations it was shown that mutations of conserved amino acids had much less influence on fast inactivation properties than mutation of the non-conserved phenylalanine to serine, F1473S [26]. Here, we extend our studies of the F1473S mutation by providing an analysis of slow inactivation and single-channel recordings. Since paramyotonic symptoms occur predominantly in a cold environment, effects of temperature on fast inactivation in WT and mutant channels were also investigated.

It has been known for a long time that local anaesthetics block Na^+ channels predominantly in their inactivated state leading to the phenomenon called use dependence [12]. Regions in the Na^+ channel that might be involved in binding of local anaesthetic drugs are thought to be the cytoplasmic end of IV/S6 [30, 31] and the interlinker connecting repeats III and IV [3, 9]. These protein regions also contain structures important for fast channel inactivation [4, 22, 24, 25, 32], thus underlining the link between channel block by local anaesthetics and fast inactivation. It is not yet clear whether the IV/S4–S5 regions are involved in the binding of local anaesthetics.

The local anaesthetic mexiletine, a lidocaine analogue, is commonly used as an antimyotonic therapeutic agent. Thus, the second aim of our study was to determine the actions of mexiletine on the F1473S mutation and contrast these to those on another mutation, G1306E, as well as to WT channels. G1306E is located within the III–IV interlinker and causes a severe form of PAM [19]. The biophysical defect of this mutation resembles that of F1473S but shows a more pronounced disruption of inactivation [25]. Whereas F1473S impairs fast inactivation, probably by somehow affecting the formation of a receptor for the proposed inactivation particle (see above), G1306E may hinder the movement of the inactivation gate itself [19, 25, 32]. Patients with either mutation respond well to treatment with mexiletine. Our investigation sought to: (1) compare the effects of mexiletine on these two Na^+ channel mutants, which cause a similar disruption of fast inactivation probably by different mechanisms; (2) determine if the IV/S4–S5 channel region is part of the binding area for local anaesthetic drugs; and (3) determine if the G1306E channel mutation decreases the binding affinity, as has been shown for two other mutants in this channel region [3, 9].

Materials and methods

Mutagenesis

Site-directed mutagenesis to generate the F1473S and G1306E mutants of the adult skeletal muscle Na^+ channel α-subunit has been described in previous reports [24, 25]. The pSELECT mutagenesis system (Promega, Madison, Wis., USA) was used and the mutants were reassembled in the pRC/CMV plasmid (Invitrogen, San Diego, Calif., USA) for transfection in the mammalian cell line HEK-293.

Transfection

To obtain cells expressing the α-subunit of WT and F1473S mutant Na^+ channels, HEK-293 cells (ATCC CRL 1573) were transfected by the calcium phosphate precipitation method [24] using the plasmids pRC/CMV containing WT and mutant cDNA. Transient expression was detected electrophysiologically 48–72 h after transfection. Oligoclonal cell lines were obtained by selection for resistance to the aminoglycoside antibiotic Geneticin (G418; Life Technologies, Scotland). Twenty hours after transfection, cells were incubated in medium supplemented with G418 (350 µg/ml). After 10–28 days, cells were pooled and used for the subsequently described electrophsiological experiments. Plasmids from at least two different cloning procedures were transfected.

Electrophysiology and data analysis

Standard *whole-cell recording* was performed using an EPC-7 voltage-clamp amplifier (EPC7, List, Darmstadt, Germany). Na^+ currents in permanently transfected cell lines were between 1 and 7 nA, whereas the endogenous Na^+ current in HEK cells ranged from 50 to 350 pA. Residual series resistance after 60–85% compensation was 0.5–2 MΩ. The voltage error due to series resistance was always <6 mV. Leakage and capacitive currents were automatically subtracted by means of a prepulse protocol (–P/4). Currents were filtered with an internal 3 kHz 4-pole Bessel filter of the amplifier and digitized at 20 kHz sampling rate using pCLAMP (Axon Instruments, Foster City, Calif., USA).

To record Na^+ currents, cells were held at –85 mV and then depolarized to various test potentials after a 300-ms prepulse to –120 mV. The time course of inactivation was best fit to a second-order exponential function, yielding two time constants of inactivation plus a constant term (I_{SS}). There was no significant difference between the slower time constant or its relative amplitude (generally <10%) between mutant F1473S and WT channels. Therefore, to describe the slowing of inactivation in the Results, only the fast time constant was used which is termed τ_h. Persistent Na^+ currents, when a steady-state was reached (I_{SS}), were determined by fits of 50-ms-long pulses to 0 mV and are given as a percentage of the initial peak current (I_{PEAK}). Steady-state inactivation was determined using 300-ms prepulses to various potentials, followed by the test pulse to 0 mV. Steady-state activation and inactivation curves were fit to standard Boltzmann functions $I/I_{max}=1/(1+\exp[(V-V_{0.5})/k_V])$, with $V_{0.5}$ being the voltage of half-maximal activation/inactivation and k_V a slope factor. Recovery from inactivation was recorded from a holding potential of –100 mV. Cells were depolarized to 0 mV for 100 ms to inactivate all Na^+ channels and then repolarized to various recovery potentials for increasing durations. The time course of recovery from inactivation was best fit to a second-order exponential function. For comparison among WT and mutant channels, only the fast recovery time constant (τ_{rec}) was used, since the slow one had a relatively small weight (<25%) and did not vary much compared to the fast one.

For *single channel recordings* cell-attached patches were held at –120 mV and depolarized to potentials ranging from –60 to 0 mV for a duration of 200 ms. Mean open times, first latencies and late channel openings were evaluated for depolarizations to –30 mV with at least 300 traces recorded per patch. Leakage and capacitive currents were eliminated by subtracting averaged and scaled records without channel activity. The number of channels in a patch was determined by inspecting traces and counting the maximum number of channels that open simultaneously [13]. First latencies and mean open times were evaluated from patches containing no more than four channels. To compare measurements from mutant and WT patches, cumulative latency distributions were corrected for the number of channels in the patch [28]. Late channel reopenings were evaluated between 90 and 190 ms after the onset of the depolarization and normalized to the average initial peak current [19].

The temperature was controlled via a water bath. If not indicated otherwise, room temperature was utilized (21.5–22.5°C). All data were analysed using a combination of pCLAMP, Excel (Microsoft), SigmaPlot (Jandel Sientific, San Raphael, Calif., USA) and our own software. For statistic evaluations, Student's *t*-test was applied. All data are shown as means ± SEM.

Solutions

The pipette ("intracellular") solution used for whole-cell recordings contained (in mM): 135 CsCl, 5 NaCl, 2 $MgCl_2$, 5 EGTA, and 10 HEPES (pH 7.4). The bathing ("extracellular") solution contained (mM): 140 NaCl, 4 KCl, 2 $CaCl_2$, 1 $MgCl_2$, 4 dextrose and 5 HEPES (pH 7.4). Mexiletine (Boehringer Ingelheim, Ingelheim am Rhein, Germany) was dissolved in deionized water and added to the bathing solutions to obtain a final concentration of 100 µM. In order to depolarize the cells and exclude any influence of resting potential in the cell-attached mode, for single-channel recordings the bathing ("intracellular") solution contained (mM): 150 KCl, 5 NaCl, 2 $CaCl_2$, 1 $MgCl_2$, 10 HEPES (pH 7.4). The pipette ("extracellular") solution contained (mM): 140 NaCl, 4 KCl, 2 $CaCl_2$, 1 $MgCl_2$, 4 dextrose, 5 HEPES (pH 7.4).

Results

Whole-cell and single-channel experiments were performed using stable cell lines expressing either F1473S mutant or WT channels (see Materials and methods). Figure 1A shows representative, superimposed whole-cell Na^+ currents for both clones. The currents recorded from the F1473S channels decayed about two times more slowly than those from the WT. The voltage dependence of the fast inactivation time constant, τ_h, is shown in Fig. 1B. For both F1473S and WT channels, τ_h was equally voltage dependent while τ_h was significantly increased for F1473S channels at all potentials investigated. Comparing the non-inactivating steady-state currents of mutant and WT channels, in 50-ms depolarizing steps, revealed a small but significant increase for F1473S channels: I_{SS}/I_{PEAK} (%) at 0 mV was 1.9±0.4% versus 0.9±0.2% for the WT, n=5 and 10, P<0.05. The steady-state inactivation curve for the mutants was shifted by 18 mV in the depolarizing direction (Fig. 1C) whereas steady-state activation was almost identical for both the mutant and normal channels (not shown, standard Boltzmann parameters for steady-state activation were: $V_{0.5}$=–17±1 mV versus –16±1 mV; k_V=–6.1±0.3 mV versus –5.9±0.3 mV, n=10). Since first latencies were also similar for both channel types (Fig. 2A, see below), F1473S had no obvious effect on channel activation. Recovery from fast inactivation was accelerated fivefold (e.g. at –100 mV τ_{rec} was 0.46±0.01 ms versus 2.7±0.2 ms, n=6 and 10, P<0.001) and its voltage dependence was shifted by about +20 mV, as for steady-state inactivation, indicating a severe destabilization of the fast inactivated state for F1473S [26].

In contrast to the marked difference in fast inactivation gating of F1473S compared with WT, slow inactivation was almost identical for both clones. Figure 1D–F shows the results obtained for steady-state slow inactivation, and the time courses of slow inactivation and its recovery. None of the evaluated parameters for the F1473S mutant channels differed significantly from those for the WT, indicating that the clinical phenotype of this mutation is probably only caused by defects in fast inactivation, which was also the case for other PC-causing mutants [11].

Single-channel studies

In order to find out the underlying mechanism accounting for the macroscopic slowing of inactivation and the increase in persistent Na^+ current, we performed single-channel measurements as described in Materials and methods (Fig. 2). Latencies to first openings were not

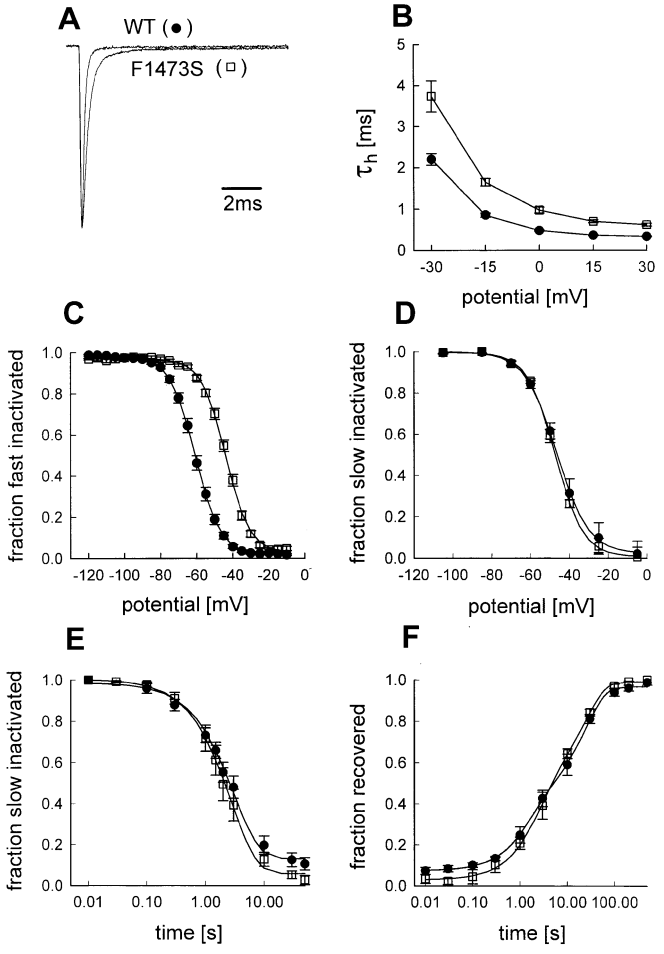

Fig. 1A–F Parameters of fast and slow inactivation of F1473S and wild-type (*WT*) Na^+ channels. Na^+ currents were elicited by applying different depolarizing test pulses after a 300-ms prepulse to –120 mV (holding potential –85 mV). **A** Superimposed representative raw whole-cell current traces for a depolarization to 0 mV for WT and mutant channels. **B** Voltage dependence of the inactivation time constant, τ_h. Values at 0 mV were 0.97±0.07 ms for F1473S versus 0.48±0.01 ms for WT, n=10,12, P<0.001. **C** Steady-state inactivation for F473S versus WT was determined using 300-ms prepulses to the potentials indicated, followed by a short test pulse to 0 mV. Lines are fits to standard Boltzmann functions. $V_{0.5}$ was –44±1 mV versus -62±1 mV, n=10–11, P<0.001; k_V was 6.6±0.2 mV versus 6.6±0.1 mV. **D** Steady-state slow inactivation was determined using 50-s prepulses to potentials indicated on the *abscissa*, followed by a 100-ms repolarizing pulse to the holding potential of –85 mV to let the channels recover from fast inactivation, and the short test pulse to 0 mV. The curves were fit using a standard Boltzmann function yielding the following parameters for F1473S versus WT: $V_{0.5}$=–48±2 mV versus –46±1 mV, k_V=6.4±0.5 mV versus 6.9±0.3 mV, n=4. **E** Time course of slow inactivation at 0 mV. Cells were held at –85 mV, depolarized to 0 mV for increasing durations indicated on the *abscissa*, repolarized for 100 ms to –85 mV to let the channels recover from fast inactivation, and then depolarized again to 0 mV to determine the fraction of slow inactivated channels. The *lines* represent fits to a first-order exponential function with the following time constants (F1473S versus WT): 4.5±1.0 s versus 3.8±0.6 s, n=8–9. **F** Recovery from slow inactivation measured at –85 mV after a 40-s conditioning pulse to 0 mV. Curves were best fit to a second-order exponential function with the following time constants (F1473S versus WT): τ_{srec1}=3.1±1.0 s versus 3.6±1.1 s, τ_{srec2}=26±2 s versus 31±6 s, relative amplitude of τ_{srec1}=51±1% versus 53±6%, n=3–6

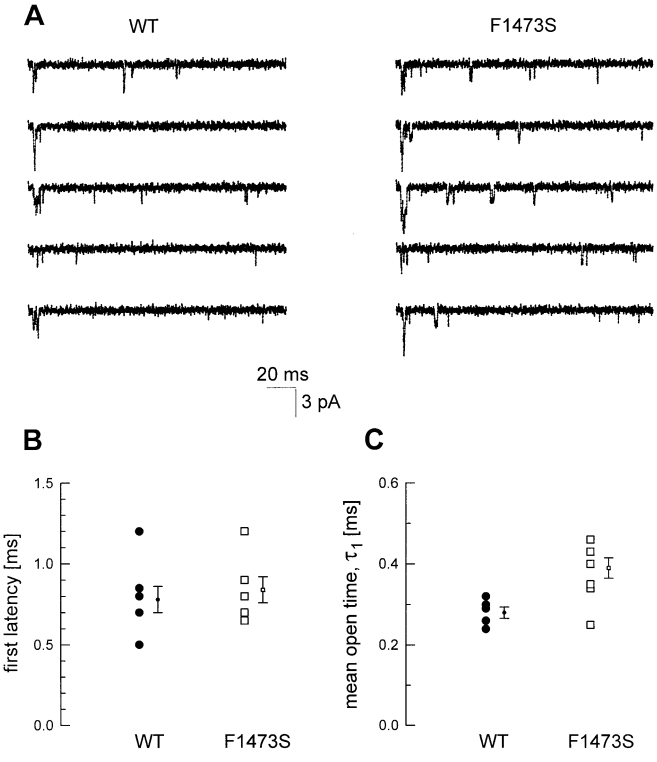

Fig. 2A–C Single-channel recordings. **A** Original current traces showing single-channel openings elicited by step depolarizations from –120 to –30 mV for WT and F1473S channels respectively. Both patches contained 4 Na^+ channels. **B** First latencies and **C** mean open times for individual data points for each recorded patch and as means ± SEMs. First latencies were 0.84±0.08 ms for F1473S channels compared to 0.78±0.08 ms for WT channels, n=6 and 8. **B** Mean open time histograms were best fit by a second-order exponential function (**C**). Shown are the fast time constants, τ_1: 0.39±0.03 ms versus 0.28±0.01 ms, n=8 and 5, P<0.02, which had relative amplitudes of 93±3% and 89±7%, respectively

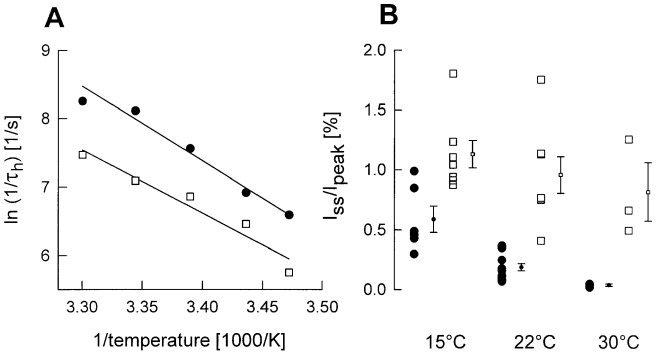

Fig. 3A, B Temperature dependence of inactivation for F1473S and WT channels. **A** Arrhenius plots of mean values of τ_h for F1473S (*open squares*) and WT (*filled circles*) channels. The corresponding activation energies (E_a) were 18.5 versus 21.8 kcal/mol, respectively. **B** Late Na^+ channel openings at different temperatures. The persistent Na^+ current between 90 and 190 ms after the onset of the depolarization was normalized to the average early peak current for at least 300 consecutive test pulses per patch. Shown are all individually measured values and averaged means ± SEM, which were as follows – 15°C: 1.13±0.11 versus 0.59±0.11%, P<0.01; 22°C: 0.96±0.15 versus 0.19±0.03%, P<0.001; 30°C: 0.81±0.24 versus 0.04±0.01%, P<0.01, n=3–13

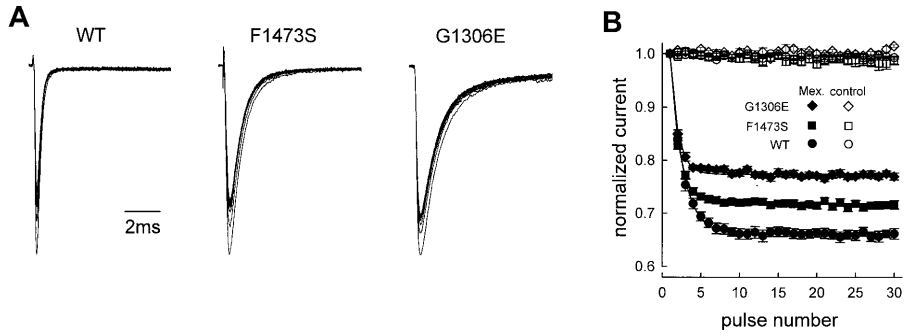

Fig. 4A, B Use-dependent block by mexiletine. To record the use-dependent block by 100 µM mexiletine, added to the bathing solution, cells were held at –120 mV and depolarized 30 times to +20 mV for 10 ms at a frequency of 10 Hz. **A** Shown are the normalized raw current traces for WT, F1473S and G1306E channels. The maximal current amplitudes were 4.7, 4.1, and 3.8 nA, respectively. **B** The decreases of peak current as a percentage of the first pulse amplitude for all three clones (*filled symbols*). The average peak current amplitude of the last 15 pulses relative to the first peak indicated a use-dependent block of 33.9±0.2, 28.4±0.1 and 23.8±0.1% for WT, F1473S and G1306 respectively (Table 1). There was no decrease in amplitude in the absence of mexiletine (*open symbols*).

significantly different for mutant versus WT channels, indicating that slowing of inactivation is not due to a delayed activation (Fig. 2B). Mean open time histograms were best fit to a second-order exponential function for each channel type. For the mutants the first time constant differed significantly from that of WT (Fig. 2C), whereas the second time constant and its weight were not different between the mutants and WT. The occurrence of late channel reopenings in a steady-state has been shown to account for a persistent macroscopic Na^+ current for many Na^+ channel mutants causing myotonia and/or paralysis [4, 5, 17, 19, 20, 24, 25]. Compatible with our whole-cell data, late channel openings were increased significantly for F1473S channels (Fig. 3B). In summary, single-channel recordings revealed an increase in mean open time and increases in the frequency of channel reopenings, causing a slowed and incomplete channel inactivation.

Effects of temperature

Cold-induced muscle stiffness and weakness is one of the key symptoms of PC. To investigate the influence of temperature on mutant and WT channels, kinetics of inactivation in the range of 15 to 30°C were compared. Lowering the temperature slowed the kinetics for both channel types as is shown by Arrhenius plots of the fast inactivation time constant, τ_h, in Fig. 3A. As was also found for other PC-causing mutations [7, 20, 33], the slopes from the plots yielded similar activation energies (E_a) for both the F1473S and the WT channels (Fig. 3A). Over a temperature range of 20°C to 30°C, the corresponding Q_{10} values were 2.9 for F1473S and 3.4 for WT channels.

For whole-cell recordings carried out at 15°C, I_{SS} was increased for both the F1473S and the WT channels: by 2.1-fold (1.9±0.4%) and 2.4-fold (4.6±0.7%) respectively. Since single-channel recordings revealed the late current more accurately, the temperature dependence of late channel reopenings was evaluated (Fig. 3B). The frequency of reopenings for mutant channels was increased at all temperatures compared to the WT ones and both channel types showed an increasing late open probability at lower temperatures.

Channel block by mexiletine

The local anaesthetic and antiarrhythmic drug mexiletine, a lidocaine analogue, is commonly used to treat the myotonic symptoms of PC and PAM [18]. To characterize and compare the blocking effects of this drug on WT, mutant F1473S and G1306E channels, we examined use-dependent block, the time course of block using a two-pulse protocol, recovery from block and effects of the drug on steady-state inactivation using a concentration of 100 µM mexiletine, which was added to the bathing solution. Effects of local anaesthetics are known to be dose dependent [3, 9, 12], including those of mexiletine [27]. Here – for comparison among WT, F1473S and G1306E channels – we only present data for a single mexiletine concentration, of 100 µM, which had a definite, well-resolved blocking effect on all three clones. Concentrations of 30 and 300 µM, as tested for a few cells expressing WT or F1473S channels, produced a less and a more pronounced block, respectively, for all parameters investigated (data not shown). All experiments were carried out using a holding potential of –120 mV. Mexiletine had no influence on the kinetics of inactivation (data not shown).

Use-dependent block

Since local anaesthetics block Na^+ channels predominantly in their inactivated state, a characteristic feature is the use-dependent or phasic block which develops cumulatively during frequent depolarizations. Cells were held at –120 mV and depolarized for 10 ms at a frequency of 1 to 10 Hz to +20 mV. Without mexiletine, there was no decrease in current amplitude using this protocol (Fig. 4B). As expected, phasic block increased with increasing

Table 1 Effects of mexiletine. This table summarizes all results shown in Figs. 4 and 5 concerning WT and mutant channel block by 100 µM mexiletine (means ± SEMs). Significant differences to WT are indicated as follows: $^{*}P<0.05$, $^{**}P<0.01$. The percentage of use-dependent block was calculated as explained in Fig. 4. The time course of block was fit to a third-order exponential function yielding the time constants for block of open channels (τ_{ob}), block of inactivated channels (τ_{ib}), and the time constant for slow inactivation (τ_{si}) which was also determined in the absence of mexiletine. The relative amplitudes of the different exponential components are indicated as a fraction of each τ. The shift in steady-state inactivation by mexiletine was determined for 500-ms prepulses. The time course of recovery from block was fit to a third-order exponential function yielding two time constants for recovery from inactivation (τ_{rec1}, τ_{rec2}), which were also determined in the absence of mexiletine, and the time constant for recovery from block by mexiletine (τ_{rmex})

Parameter	G1306E	F1473S	WT
Use-dependent block:	*n*=12	*n*=21	*n*=14
Steady-state level as a percentage of first peak	23.8±0.1**	28.4±0.1**	33.9±0.2
Time course of block:	*n*=11	*n*=9	*n*=11
τ_{ob} (ms)	0.8±0.1	1.2±0.2	0.7±0.1
τ_{ib} (ms)	83.5±7.7	72.1±8.5	80.3±5.5
τ_{si} (s)	2.7±0.8	4.0±0.7	3.4±0.3
Fraction τ_{ob} (%)	16±1	18±1	16±2
Fraction τ_{ib} (%)	42±3**	47±2*	60±3
Fraction τ_{si} (%)	42±2**	35±1*	24±2
Slow inactivation in the absence of mexiletine:	*n*=5	*n*=6	*n*=3
τ_{si} (s)	3.8±1.8	6.1±2.1	6.0±1.7
Steady-state inactivation V1/2 (mV):	*n*=8, 6	*n*=3, 14	*n*=8, 13
Control	–51.8±1.7	–46.4±1.0	–64.5±0.9
Mexiletine	–59.5±1.7	–53.2±1.0	–70.0±1.3
Shift (mV)	7.7	6.8	5.5
Recovery from block:	*n*=5	*n*=7	*n*=9
τ_{rec1} (ms)	3.7±0.5	1.2±0.6	0.8±0.4
τ_{rec2} (ms)	17.4±3.5	9.6±2.3	8.5±2.1
τ_{rmex} (ms)	539±51*	523±35*	693±31
Fraction τ_{rec1} (%)	23±3	14±2	17±3
Fraction τ_{rec2} (%)	20±3	18±2	17±3
Fraction τ_{rmex} (%)	57±3*	68±1	66±2
Recovery from inactivation in the absence of mexiletine:	*n*=4	*n*=4	*n*=5
τ_{rec1} (ms)	1.4±0.1	0.4±0.1	1.6±0.1
τ_{rec2} (ms)	14.6±1.1	10.1±1.3	19.2±2.4
Fraction t1rec1 (%)	70±3	81±3	75±4

frequency (results not shown). The steady-state level of block, reached after a few depolarizations, was significantly reduced for G1306E >F1473S versus WT channels as shown in Fig. 4 and Table 1 for 10-ms test pulses at 10 Hz.

Time course of mexiletine block

The time course of mexiletine block was investigated by a two-pulse protocol with a variable conditioning prepulse to +20 mV followed by a recovery period to –120 mV, to let the channels recover from fast inactivation, and the short test pulse to +20 mV. The recovery interval was set to 100 ms, since this was the time period separating recovery from fast inactivation and recovery from block (see Fig. 5D). In the absence of mexiletine, this protocol revealed the time course of slow inactivation, which was similar for WT and for both types of channel mutations (Fig. 5A, Table 1). The time constants are similar to those shown in Fig. 1, although the pulse protocol was slightly different. For G1306E channels, it has been shown by Hayward and colleagues [11] that slow inactivation is not different from that of WT. The time course of mexiletine block was bi-exponential, with a fast time constant that presumably represents open state block, τ_{ob}, and a slow one representing inactivated state block, τ_{ib}. The time course of block was followed by slow inactivation with similar time constants as in the absence of mexiletine, τ_{si}. The relative weight of τ_{ib} was significantly reduced for both mutations compared to WT, whereas the time constants were almost identical for all three clones (Fig. 5A, Table 1).

Recovery from mexiletine block

Recovery from mexiletine block was investigated by applying a 200-ms conditioning pulse to +20 mV followed by the recovery period to –120 mV for increasing durations and the short test pulse to +20 mV (Fig. 5C,D). The duration of the conditioning pulse was restricted to 200 ms, because at this point of time the mexiletine block had almost fully developed and the contribution of slow inactivation was minimal (see Fig. 5A). The interpulse interval was 10 s, so that complete recovery from block was ensured. Figure 5C shows recovery from inactivation under the same conditions in the absence of mexiletine. As was already found for a 100-ms conditioning pulse (Fig. 1), the time course of recovery had two exponential time constants (τ_{rec1}, τ_{rec2}, Table 1). In the presence of mexiletine, an additional slow time con-

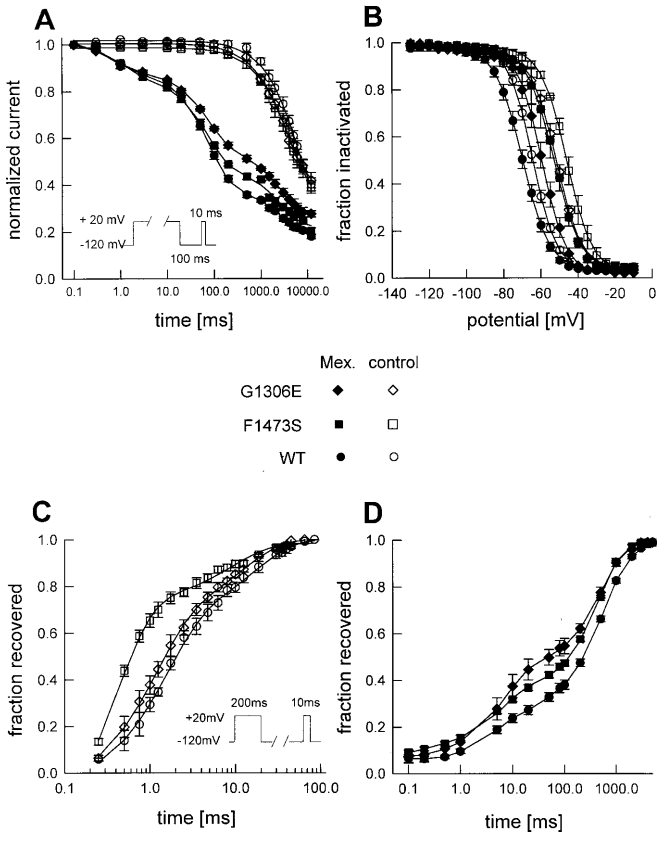

Fig. 5A–D Time course of block, shift in steady-state inactivation and recovery from block by mexiletine. All original data are listed in Table 1. The pulse protocols used are indicated as *insets*. Mexiletine (100 µM) was added to the bathing solution. **A** Time course of blockade as studied by the indicated two-pulse protocol. *Lines* represent fits to a third-order exponential function. **B** The shift in steady-state inactivation induced by mexiletine (500 ms prepulse duration) was similar for all three clones. *Lines* represent fits to standard Boltzmann functions. **C** Recovery from inactivation at –120 mV after a 200-ms conditioning pulse to +20 mV in the absence of mexiletine. *Lines* represent fits to a second-order exponential function. **D** Recovery from inactivation and from mexiletine block using the same pulse protocol as in **C**. *Lines* represent fits to third-order exponentials

stant was found describing recovery from mexiletine block (τ_{rmex}), while the faster time constants remained similar to those measured in the absence of mexiletine. τ_{rmex} was slightly but significantly decreased for both F1473S and G1306E mutations relative to the WT (Fig. 5D, Table 1). Corresponding to the amplitude relationships during the time course of mexiletine block, the relative weight of τ_{rmex} was significantly reduced for G1306E>F1473S versus WT channels.

Shift in steady-state inactivation via mexiletine

Stabilization of the inactivated state by binding of local anaesthetics is represented by a hyperpolarizing shift in steady-state inactivation, which also yields a measure of the affinity of the drug to the inactivated state [2, 9]. To ensure adequate blocking effects of 100 µM mexiletine, without affecting slow inactivation too much, we chose a prepulse duration of 500 ms followed by test pulses to +20 mV. Under these conditions similar shifts of steady-state inactivation were induced by mexiletine for all three clones (Fig. 5B, Table 1), suggesting that the affinity of mexiletine for the inactivated state was not substantially altered by either mutation.

Discussion

The F1473S mutation within the α-subunit of the human skeletal muscle Na^+ channel causes a classic clinical phenotype of PC. The mutation shows a similar biophysical defect compared to other PC-causing mutations, in particular a slowing of inactivation and an accleration of recovery from inactivation [7, 20, 26, 33]. A slowed current decay may be a pathophysiological explanation for paradoxical myotonia, since most of the abnormal, depolarizing inward Na^+ current flows during an action potential, i.e. during exercise [20]. The acceleration of recovery from inactivation contributes to myotonia by shortening the refractory period after an action potential. At the single-channel level, the slowed and incomplete inactivation could be explained by prolonged mean open times and an increased frequency of channel reopenings.

The temperature sensitivity of F1473S was similar to that of WT channels as revealed by analysis of the fast inactivation time constant and late channel reopenings (corresponding to the macroscopic persistent Na^+ current). However, mutant channels displayed an increased persistent Na^+ current and a slower inactivation at all temperatures investigated, while these inactivation defects increased with further cooling. We therefore propose that both the slowing of Na^+ channel inactivation and a persistent Na^+ current have to exceed a certain threshold to elicit phenotypic myotonic and/or paralytic symptoms in a cold environment [20].

Effects of mexiletine

The influences of two Na^+ channel mutations, the F1473S (located in the IV/S4–S5 loop) and G1306E (located within the inactivation gate, the III–IV linker) on channel block by mexiletine induced a reduced phasic block, a decrease in the fraction of channels blocked in the inactivated state upon a two-pulse protocol, and a slight increase in the rate of recovery from block. The differences to WT channels were more pronounced for G1306E, which displays a more severe disruption of inactivation than the F1473S mutant, namely a threefold slowing of inactivation and a threefold increase in persistent current [25] compared to a twofold change in both parameters for F1473S. The reduction in phasic block may be explained by several different mechanisms: (1) by slowed inactivation, since during a 10-ms depolarizing pulse more WT than mutant channels were in an inactivated state, which is the state that has the

highest affinity for local anaesthetics; (2) by an acceleration of recovery from block; and (3) by the reduction in the fraction of blocked channels which is revealed by the two-pulse experiment. Although the reduced fraction of blocked channels could reflect a decreased affinity for mexiletine, the almost identical effect of mexiletine on steady-state inactivation of WT and mutant channels argues against affinity being significantly changed. For a different mutation within the III–IV interlinker, the T1313 M exchange, Fan and colleagues [9] found a reduced affinity for the inactivated state. Using almost the same pulse protocol as in this study, they reported no shift in steady-state inactivation with 100 µM lidocaine for T1313M; whereas for WT channels the shift was similar to the one measured in our study.

A different explanation for the reduced fraction of blocked channels could be incomplete inactivation. Mutant channels showed an increase of 1–2% of the persistent, non-inactivating Na^+ current. This persistent current is caused by reopenings of Na^+ channels, either in the form of long channel bursts or as single events, which is best explained by "modal gating" [5, 20, 24, 29]. Occasionally the channels enter a gating mode in which they frequently reopen from the inactivated state. The fraction of channels being in such a non-inactivating mode could be much higher than the relation of the persistent to the peak current, since channels in the non-inactivating mode do not open 100% of the time. If mexiletine can only bind to channels in the normal gating mode, this might explain the relatively large decrease in the fraction of blocked channels in the two-pulse experiment.

Clinical mechanism of action of mexiletine

The electrophysiological correlate of myotonia is repetitive action potentials, regardless of the underlying reason, namely a Cl^- or a Na^+ channel defect. Because of the use-dependent channel block, the generation of a single action potential, and thus the excitability of a muscle fibre, is not changed in the presence of low concentrations of mexiletine. However, the generation of repetitive action potentials is suppressed. This antimyotonic effect is considered rather unspecific. However, additional effects on Na^+ channels might be relevant too. The persistent Na^+ current, caused by reopenings, should be reduced by mexiletine, as has been proven for mutant cardiac Na^+ channels [1], and the inactivated state is stabilized by a hyperpolarizing shift in steady-state inactivation and a slowing of recovery from inactivation.

Acknowledgements We thank Dr. Paul A. Iaizzo for his comments on the manuscript and Ms. Ursula Pika-Hartlaub for performing excellent cell culture. This work was supported by the Deutsche Forschungsgemeinschaft (Le481/3–3), the Muscular Dystrophy Association and the Deutsche Gesellschaft für Muskelkranke.

References

1. An RH, Bangalore R, Rosero SZ, Kass RS (1996) Lidocaine block of LQT-3 mutant human Na^+ channels. Circ Res 79: 103–108
2. Bean BP, Cohen CJ, Tsien RW (1983) Lidocaine block of cardiac Na^+ channels. J Gen Physiol 81:613–642
3. Bennett PB, Valenzuela C, Chen LQ, Kallen RG (1995) On the molecular nature of the lidocaine receptor of cadiac Na^+ channels – modification of block by alteration in the α-subunit III-IV interdomain. Circ Res 77:584–592
4. Cannon SC, Strittmatter SM (1993) Functional expression of Na^+ channel mutations identified in families with periodic paralysis. Neuron 10:317–326
5. Cannon SC, Brown RH Jr, Corey DP (1991) A Na^+ channel defect in hyperkalemic periodic paralysis: potassium-induced failure of inactivation. Neuron 6:619–626
6. Catterall WA (1995) Structure and function of voltage-gated ion channels. Annu Rev Biochem 64:493–531
7. Chahine M, George AL, Zhou M, Ji S, Sun W, Barchi RL, Horn R (1994) Na^+ channel mutations in paramyotonia congenita uncouple inactivation from activation. Neuron 12:281–294
8. Cummins TR, Sigworth FJ (1996) Impaired slow inactivation of mutant Na^+ channels. Biophys J 71:227–236
9. Fan Z, George AL, Kyle JW, Makielski JC (1996) Two human paramyotonia congenita mutations have opposite effects on lidocaine block of Na^+ channels expressed in a mammalian cell line. J Physiol (Lond) 496:275–286
10. Filatov GN, Nguyen TP, Kraner SD, Jarchi RL (1998) Inactivation and secondary structure in the D4/S4–5 region of the SkM1 sodium channel. J Gen Physiol 111:703–715
11. Hayward LJ, Brown RH Jr, Cannon SC (1997) Slow inactivation differs among mutant Na^+ channels associated with myotonia and periodic paralysis. Biophys J 72:1204–1219
12. Hille B (1992) Mechanisms of block. In: Hille B (ed) Ionic channels of excitable membranes, 2nd edn. Sinauer, Sunderland, Mass., pp 390–422
13. Horn R (1991) Estimating the number of channels in patch recordings. Biophys J 60:433–439
14. Lehmann-Horn F, Rüdel R (1997) Channelopathies: contributions to our knowledge about voltage-gated ion channels. News Physiol Sci 12:105–112
15. Lehmann-Horn F, Küther G, Ricker K, Grafe P, Ballanyi K, Rüdel R (1987) Adynamia episodica hereditaria with myotonia: a non-inactivating Na^+ current and the effect of extracellular pH. Muscle Nerve 10:363–374
16. Lehmann-Horn F, Rüdel R, Ricker K (1987) Membrane defects in paramyotonia congenita (Eulenburg). Muscle Nerve 10:633–641
17. Lehmann-Horn F, Iaizzo PA, Hatt H, Franke C (1991) Altered gating and conductance of Na^+ channels in hyperkalemic periodic paralysis Pflügers Arch 418:3 297–299
18. Lehmann-Horn F, Engel AG, Ricker K, Rüdel R (1994) The periodic paralyses and paramyotonia congenita. In: Engel AG, Franzini-Armstrong (eds) Myology, 2nd edn. McGraw-Hill, New-York pp 1303–1334
19. Lerche H, Heine R, Pika U, George AL Jr, Mitrovic N, Browatzki M, Weiss T, Rivet-Bastide M, Franke C, Lomonaco M, Ricker K, Lehmann-Horn F (1993) Human Na^+ channel myotonia: slowed channel inactivation due to substitutions for a glycine within the III-IV linker. J Physiol (Lond) 470:13–22
20. Lerche H, Mitrovic N, Dubowitz V, Lehmann-Horn F (1996) Paramyotonia congenita: the R1448P Na^+ channel mutation in adult human skeletal muscle. Ann Neurol 39:599–608
21. Lerche H, Peter W, Fleischhauer R, Pika-Hartlaub U, Malina T, Mitrovic N, Lehmann-Horn F (1997) Role in fast inactivation of the IV/S4-S5 loop of the human muscle Na^+ channel probed by cysteine mutagenesis. J Physiol (Lond) 505:345–352
22. McPhee JC, Ragsdale DS, Scheuer T, Catterall WA (1995) A critical role for transmembrane segment IVS6 of the Na^+ channel alpha subunit in fast inactivation. J Biol Chem 270:12025–12034

23. McPhee JC, Ragsdale DS, Scheuer T, Catterall WA (1998) A critical role for the S4–S5 intracellular loop in domain IV of the sodium channel alpha-submit in fast inactivation. J Biol Chem 273:1121–1129
24. Mitrovic N, George AL Jr, Heine R, Wagner S, Pika U, Hartlaub U, Zhou M, Lerche H, Fahlke C, Lehmann-Horn F (1994) K^+ aggravated myotonia: The V1589M mutation destabilizes the inactivated state of the human muscle Na^+ channel. J Physiol (Lond) 478:395–402
25. Mitrovic N, George AL Jr, Lerche H, Wagner S, Fahlke C, Lehmann-Horn F (1995) Different effects on gating of three myotonia-causing mutations in the inactivation gate of the human muscle Na^+ channel. J Physiol (Lond) 487:107–114
26. Mitrovic N, Lerche H, Heine R, Fleischhauer R, Pika-Hartlaub U, Hartlaub U, George AL Jr, Lehmann-Horn F (1996) Role in fast inactivation of conserved amino acids in the IV/S4-S5 loop of the human muscle Na^+ channel. Neurosci Lett 213:1–4
27. Ono M, Sunami A, Sawanobori T, Hiraoka M (1994) External pH modifies sodium channel block by mexiletine in guinea pig ventricular myocytes. Cardiovasc Res 28:973–979
28. Patlak J, Horn R (1982) Effects of *N*-bromacetamide on single-channel currents in excised membrane patches. J Gen Physiol 79:333–351
29. Patlak J, Ortiz M (1986) Two modes of gating during late Na^+ channel currents in frog sartorius muscle. J Gen Physiol 87: 305–326
30. Qu YS, Rogers J, Tanada T, Scheuer T, Catterall WA (1995) Molecular determinants of drug access to the receptor site for antiarrhytmic drugs in the cardiac Na^+ channel. Proc Natl Acad Sci USA 92:11839–11843
31. Ragsdale S, McPhee J, Scheuer T, Catterall W (1994) Molecular determinants of state-dependent block of Na^+ channels by local anesthetics. Science 265:1724–1728
32. West JW, Patton DE, Scheuer T, Wang Y, Goldin AL, Catterall WA (1992) A cluster of hydrophobic amino acid residues required for fast Na^+ channel inactivation. Proc Natl Acad Sci USA 89:10910–10914
33. Yang N, Ji S, Zhou M, Ptácek LJ, Barchi RL, Horn R, George AL Jr (1994) Na^+ channel mutations in paramyotonia congenita exhibit similar biophysical phenotypes in vitro. Proc Natl Acad Sci USA 91:12785–12789
34. Yang N, George AL Jr, Horn R (1996) Molecular basis of charge movement in voltage-gated Na^+ channels. Neuron 16:113–122